Rigidity phase transition in granular packings

Einat Aharonov[1] and David Sparks[2]
[1]*Lamont-Doherty Earth-Observatory, Columbia University, Route 9W, Palisades, New York 10964*
[2]*Department of Geology and Geophysics, Texas A&M University, College Station, Texas 77843*
(Received 12 May 1999)

We numerically model two-dimensional systems of granular aggregates confined between two rough walls and demonstrate that at a critical grain volume fraction ν_c an abrupt rigidity transition occurs. The transition has first-order characteristics, although the elastic constants undergo a second-order transition. Densely packed grains, with a volume fraction $\nu > \nu_c$, display an elastic-plastic rheology. Loose packings, with $\nu < \nu_c$, display gaslike characteristics. It is shown that when the volume fraction is allowed to change freely (applying a constant normal stress to the walls), it evolves spontaneously to ν_c under a wide range of boundary stress values, demonstrating that the phase boundary is an attractive critical state. [S1063-651X(99)01911-X]

PACS number(s): 45.70.Ht, 05.65.+b

I. INTRODUCTION

Granular media are fundamental, yet not well understood, complex systems with wide ranging applications to technological and natural systems. In recent years there has been much work on granular dynamics, with emphasis on how behavior of grain aggregates may resemble solids, liquids, or gases (e.g., Ref. [1]). Already Reynolds in 1885 [2] noted that loosely packed sands deform easily as fluids while dense packings resist shear as solids. The two phases are traditionally treated separately by ''kinetic-gas'' approaches for loosely packed grains [3–5] and elastoplastic (often using associated plasticity [6]) theories for dense soils, but the limits on the validity of each of these end-member models is not understood. The very different behavior of low and high density granular systems has been seen in both experiments [7,8] and simulations [9] of sheared granular material, which have shown a sharp increase in stresses as the solid fraction of the system is increased beyond a critical limit. However, solidlike and gaslike regions often coexist within the same flowing system [10], particularly where boundary layers form near walls (e.g., Refs. [11, 12]), or where gravitational forces are important [13,14]. This coexistence of two differently behaving phases makes it necessary to understand the nature of the transition, and the phase space of granular materials. In this paper we numerically investigate the transition between solidlike and gaslike behavior in two-dimensional granular aggregates, both in static packings and under shear. We find that the phase transition between gaslike and solidlike behavior is marked by temporal and/or spatial coexistence of the two phases, and that the granular system is attracted by the phase boundary.

We numerically model grain aggregates using a version of the popular ''discrete element method'' [15] which treats grains as inelastic disks with rotational and translational degrees of freedom, and has the capability of simulating both elastoplastic (e.g., Ref. [16]) and gaslike (e.g., Ref. [14]) rheology. In our model two grains of radius R_i and R_j undergo an inelastic interaction when the distance separating them r_{ij} is less than the sum of their radii. During the interaction the ith grain experiences a contact force that has both shear and normal components:

$$F_{ij}(t) = [k_n(R_i + R_j - r_{ij}) - \gamma m_{ij}(\dot{\mathbf{r}}_{\mathbf{ij}} \cdot \hat{\mathbf{n}})]\hat{\mathbf{n}} + \{\min[k_s \Delta_s, \mu(\mathbf{F} \cdot \hat{\mathbf{n}})]\}\hat{s}, \quad (1)$$

where $\hat{\mathbf{n}} = (\mathbf{r}_{ij} \cdot \hat{\mathbf{x}}, \mathbf{r}_{ij} \cdot \hat{\mathbf{y}})/r_{ij}$, $\hat{\mathbf{s}} = (\mathbf{r}_{ij} \cdot \hat{\mathbf{y}}, -\mathbf{r}_{ij} \cdot \hat{\mathbf{x}})/r_{ij}$, are the unit vectors in the normal and tangential directions respectively. k_n, k_s are the normal and shear elastic constants, m_{ij} is the harmonic mean of the two grain masses, m_i and m_j, γ is a damping coefficient that ensures inelasticity of the interaction, μ is the surface friction coefficient, and Δs is the shear displacement since the initial contact of two grains. Force is integrated through time to calculate grain position, velocity and rotation, using a Verlet algorithm [17]. Energy loss is governed by a normal restitution coefficient $e_n = \exp(-\gamma t_{\mathrm{col}}/2)$, where $t_{\mathrm{col}} = \pi(k_n/m_{ij} - \gamma^2/4)^{-1/2}$ is the collision time, and by frictional work which depends on the amount of slip between grain surfaces and the frictional shear force μF_n. Distance is measured in units of average disk diameter $x_0 = 2\overline{R}$, time is scaled by the undissipated elastic wave travel time across this distance scale $t_0 = \sqrt{\overline{m}/k_n}$, velocity is scaled by the elastic wave speed $v_0 = x_0/t_0$, and stress by $\sigma_0 = k_n/x_0$. In simulations presented here $k_n = 1$, $k_s = 0.5$ and $m_i = (R_i/\overline{R})^2$ (so that grains of average radius have a mass of 1). The systems are highly damped, with $\gamma = 1$, corresponding to a normal restitution coefficient of about 0.3.

In this paper we discuss three related sets of simulations. The first set examines the general characteristics of static granular aggregates after compaction between two parallel horizontal plates. The second and third sets of simulations look at the behavior of the same confined aggregates during shear using two different boundary conditions: constant distance between shearing walls, termed constant volume boundary conditions (CVBCs), and constant normal stress applied to the wall, termed constant force boundary conditions (CFBCs). The simulations included no gravitational forces, and were performed in square systems with n disks. The top and bottom boundaries of the box were composed of grains glued together to form rigid rough walls of length l (Fig. 1). The system was periodic in the horizontal direction. Polydispersivity was introduced to discourage ordering effects: grain radii were randomly drawn from a Gaussian dis-

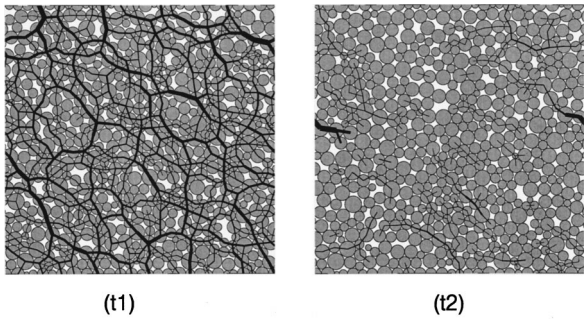

FIG. 1. Representative instantaneous grain stresses and configurations during shear (here $\nu=10^{-3}v_0$), in a CVBC, 24×24 system, with $\mu=0.5$, at times (t_1) and (t_2). A line is drawn through stressed contacts. Line thickness is proportional to normal stress on the contact, and is scaled to the largest value in the frame. The system shown here has $\nu=0.80\approx\nu_c$, and thus exhibits ''solidlike'' and ''gaslike'' behaviors intermittently during shearing: At (t_1), it is ''jammed'' with system-spanning stress chains. At time (t_2), the system is ''loose,'' with only local stress clusters. Systems with $\nu>\nu_c$ always look similar to the snapshot in $(t1)$, while those with $\nu<\nu_c$ always look similar to $(t2)$.

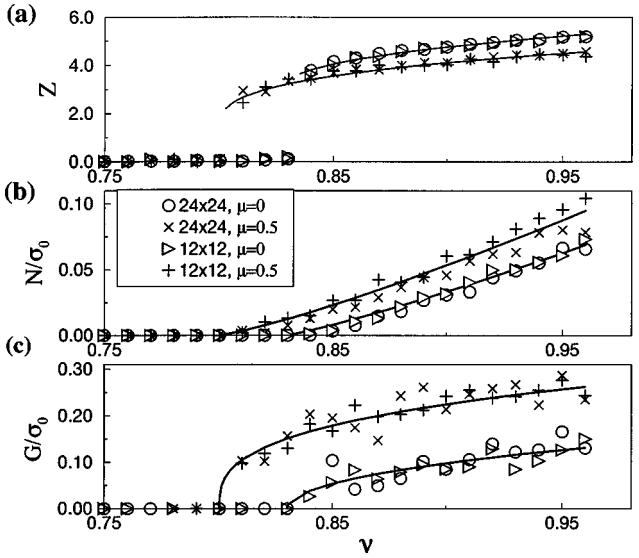

FIG. 2. Results from CVBC simulations of static 12×12 and 24×24 grain packings as a function of solid fraction ν, for smooth, $\mu=0$, and frictional, $\mu=0.5$, grains (a) Z, average coordination number per interior grain, (b) N/σ_0, scaled normal stress exerted on horizontal walls, (c) G/σ_0, scaled shear modulus of the aggregate. Solid curves are theoretical predictions, as explained in the text.

tribution that peaks at $\overline{R}$, with a standard deviation of $\overline{R}$, clipped at $0.25\overline{R}$ and $2.0\overline{R}$. The systems were initiated as tall loosely packed boxes, which were compacted vertically by normal stresses to a predetermined height l. After compaction the top and bottom walls were allowed to move freely in the horizontal direction to relax shear forces. Using CVBCs unrelaxed normal forces were maintained on the walls, since we did not allow the walls to move vertically. Global rearrangements during compaction and relaxation ensure a (local) minimal energy configuration, as would occur during natural compaction.

II. TWO-DIMENSIONAL GRAIN PACKINGS

After compaction and relaxation we measured properties of static configurations (by static we mean velocities have decayed to $10^{-8}v_0$ or smaller) at different prescribed densities, or solid fractions, $\nu=\Sigma_{i=1}^{n}\pi R_i^2/l^2$, ranging between 0.75 to 0.96. These two-dimensional (2D) solid fractions can be mapped to 3D volume fractions of 0.49 to 0.71, using a relationship between packings of circles and spheres ($\nu_{3D}=4\nu_{2D}^{3/2}/3\pi^{1/2}$ [18]). For each value of the solid fraction, simulations were performed for two different values of the friction coefficient ($\mu=0.0$ and $\mu=0.5$) and system size (12×12 and 24×24). Simulations performed at the same conditions with different random grain assemblages produced very similar results.

Figure 2 presents three measured parameters plotted as a function of solid fraction: (a) the number of grains touching (i.e., exerting a force on) a grain, averaged over the interior of the box, termed the coordination number Z, (b) the normal stress (normal force per unit length) N operating on the upper and lower confining walls, and (c) the system's shear modulus G. All measurements show an abrupt change in behavior at a critical volume fraction ν_c, which depends on the coefficient of friction prescribed between the grains, but not on the system size. The coordination number is approximately zero for $\nu<\nu_c$. At ν_c the coordination number abruptly jumps indicating a first-order phase transition. Above ν_c Z increases as an empirical power law, $Z=Z_{c\mu}+b_\mu(\nu-\nu_{c\mu})^{\alpha_\mu}$, where the subscript μ denotes fits to simulations with different friction values. Power-law fits (in solid curves) yield $Z_{c0}=3.2\pm0.5$, $b_0=5.6\pm0.5$, $\nu_{c0}=0.83\pm0.01$, $\alpha_0=0.48\pm0.1$ and $Z_{c0.5}=1.7\pm0.5$, $b_0=5.8\pm0.5$, $\nu_{c0.5}=0.8\pm0.01$, $\alpha_{0.5}=0.36\pm0.1$, for simulations performed with $\mu=0$ and $\mu=0.5$, respectively. Critical behavior with values of $\nu_{c0}=0.82\pm0.02$ were previously obtained for hard frictionless disks [19], and viscoelastic 2D bubbles [20] for monodispersed and polydispersed systems, demonstrating that ν_c is fairly independent of the disk size distribution, and the interaction law in the absence of friction. This value of $\nu_{c0}=0.82\pm0.02$ was shown to mark the upper limit of compacity of disordered packings of smooth hard monosized and polysized disks [19]; for $\nu>\gamma_{c0}$ there appears long-range order in disk positions. The difference in Z_c, ν_c, and α between frictional and smooth grains occurs because frictional grains tend to ''stick,'' and thus cannot achieve the lower energy configuration of smooth disks. The transition density for frictional grains corresponds to a 3D volume fraction of 0.54. Experiments [8] confirm that immense stiffening of rapidly shearing frictional grain aggregates occurs at $\nu_c\approx0.54$.

The fact that N and Z [Figs. 2(a), 2(b)] are zero for $\nu<\nu_c$, indicates that grains can rearrange so that they are not touching, a state with no stored elastic energy. In systems that are denser than ν_c, packing constraints lead to contacts between grains so that there is residual elastic potential energy. The elastic repulsion forces at these contacts exert normal stresses on the walls which follow $N\propto Z(\nu-\nu_c)$ (shown in solid lines). This is physically expected because the normal stress must be proportional to the number of elastic con-

tacts per disk, and to the compression of these contacts. This form is a slightly modified (to account for the phase transition) form of predictions from standard models of densely packed elastic disks [21].

The appearance at ν_c of a nonzero value of the shear modulus G [Fig. 2(c)] identifies this transition as a macroscopic rigidity transition. G is obtained by imposing a small homogeneous shear step strain of a magnitude ϵ and measuring the resulting shear stress on the walls σ ($G=\sigma/\epsilon$ is independent of ϵ for $\epsilon<10^{-4}$, here we use $\epsilon=10^{-5}$). The procedure follows that outlined in Ref. [20]. Physically, the shear modulus, which is a material property, should depend on average number of elastic contacts per disk, i.e., $G\propto Z$ (solid curves), yet not on the amount of compression on these contacts, which is imposed by the boundary strain. In fact we find that $G\propto(Z-Z_c)\propto(\nu-\nu_c)^{\alpha}$, consistent with an expected second order transition of the elastic constants [22].

A similar transition at the onset of rigidity percolation was predicted theoretically [23] and numerically [24], in central-force network models. These models predict that the density of the system-spanning rigid cluster, P_∞, undergoes a discontinuous jump at a critical rigidity percolation density p_c, indicating a first-order phase transition of the form $P_\infty = a+b(p-p_c)^{\alpha}$. In our simulations, the average coordination number Z is the order parameter for this first-order transition. Meanwhile the elastic constants, describing the mechanical strength of the system, increase continuously from zero at the transition, with a form $(p-p_c)^{\alpha}$ characteristic of a second-order transition.

III. SHEAR OF GRANULAR PACKINGS

A. Constant volume boundary condition

To investigate the manifestation of the transition and its effects on the dynamic behavior of grains we conducted a set of simulations in which the 24×24 configurations were sheared in couette flow. Here we show results of simulations with $\mu=0.5$. (Nonfrictional grains and other values of friction showed similar behavior except the transition occured at the value $\nu_{c\mu}$ identified by the static simulations and are thus not presented.) The upper wall was translated horizontally at a constant velocity ($v=10^{-3}v_0$) while l was kept constant, maintaining CVBCs. We observe different behavior as a function of the solid fraction: In configurations with $\nu<\nu_{c0.5}\approx0.80$, momentum was transferred from the wall to interior grains mostly via short-lived collisions, resulting in spiky fluctuations in the time series of stress measured on the wall σ and the mean coordination number in box Z (Fig. 3). Stresses are transmitted only within local clusters [as in Fig. 1 ($t2$)]. The power spectra $S(\omega)$ of the stress fluctuations time series $\sigma(t)$ approaches white noise, demonstrating the uncorrelated nature of stress transfer [Fig. 4(a) for $\nu=0.74,0.78$]. Also there are no apparent temporal correlations in $\sigma(t)$, as seen in the auto-correlation function $C(\Delta t)$, where Δt is the time-lag [Fig. 4(b)].

For dense packings, with $\nu>\nu_{c0.5}$, grains interact via long-lasting contacts. Global motion is characterized by elastic-plastic cycles: clusters of grains in contact accumulate recoverable elastic strain, but when stresses become too great, grains suddenly rearrange to relieve the stress. Continued shearing then begins accumulation of elastic strain on the new grain arrangement. This behavior leads to a stick-slip stress time series (Fig. 3). Long clusters of these grains in contact form system-spanning ''stress chains'' that transmit forces from the boundaries into the interior [as in Fig. 1 ($t1$)]. The stress fluctuation power spectra $S(\omega)$ for $\nu>\nu_{c0.5}\approx0.80$ varies as ω^{η}, where $\eta\sim-2$, as in Fig. 4(a), indicating long-time correlations [as observed in Fig. 4(b) for

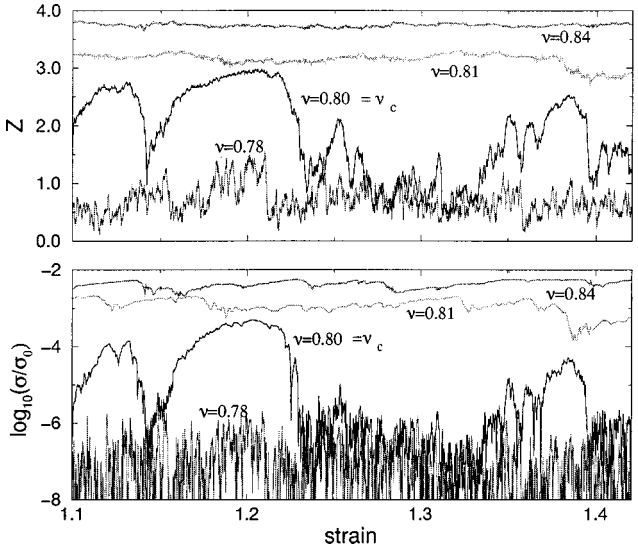

FIG. 3. Representative portions of time series of (a) mean coordination number in box Z and (b) shear stresses σ measured on wall, plotted against strain, for four CVBC 24×24 systems with different ν values, with $\mu=0.5$, sheared at $v=10^{-3}$. The time series for the simulation with $\nu=\nu_c=0.80$ shows that the system oscillates between solidlike ($\nu>\nu_c$) and gaslike ($\nu<\nu_c$) values.

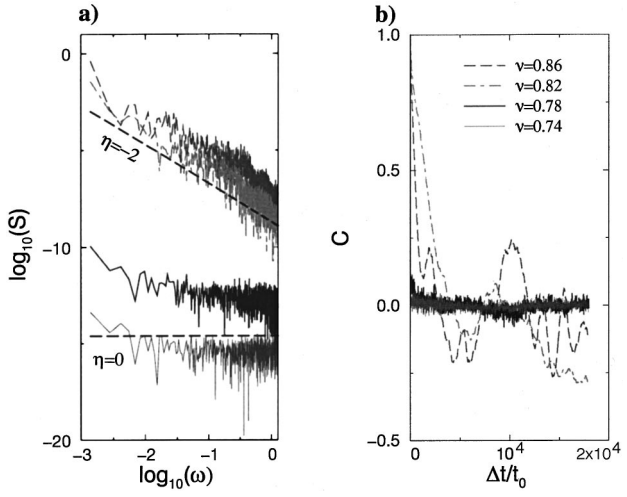

FIG. 4. (a) Power spectra $S(\omega)$ from the time series of shear stress measured on wall $\sigma(t)$, plotted as function of frequency ω, for four CVBC 24×24 systems with different ν values, with $\mu=0.5$, sheared at $v=10^{-3}$. $S(\omega)\sim\omega^{\eta}$, where for dense systems $\eta\sim-2$, and for loosely packed ($\nu=0.74$, 0.78) systems $\eta\to0$. (b) Temporal autocorrelations $C(\Delta t)$ of the stress time series $\sigma(t)$, showing long-time correlations in the dense systems. The characteristic scales imply correlations for shear strains of 1–10 grain diameters (corresponding to time lags of $\Delta t\sim10^3-10^4t_0$, respectively). The curves for the two loosely packed systems overlap, with $C(\Delta t)\approx0$.

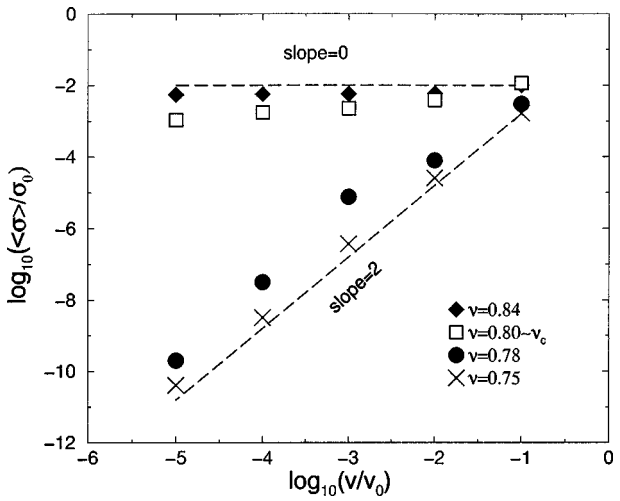

FIG. 5. Temporally averaged shear stresses measured on wall as function of shearing velocities of the upper wall, for four CVBC 24×24 systems with different ν values, with $\mu=0.5$. A different functional dependence on velocity is measured above and below the phase transition.

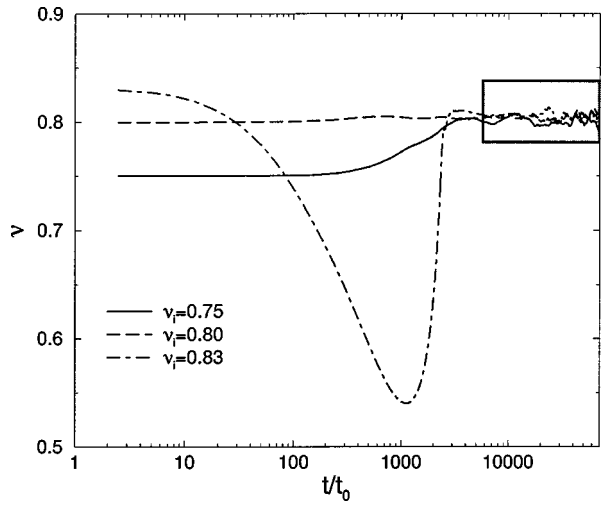

FIG. 6. Solid fraction versus time, for 3 different packings initiated with 3 different solid fractions ($\nu_i=0.75,0.80,0.83$), representing undercompacted, stable, and overcompacted packings respectively. The systems were sheared at $v=10^{-3}v_0$, and confined by $N_e=10^{-4}\sigma_0$ under CFBC. During shear the solid fraction progresses to a steady state with fluctuations around the mean (as seen within the box), independent of the initial porosity. The initially over-compacted packing ($\nu_i=0.83$) briefly overshoots the steady-state value due to inertial effects during relaxation of elastic stored energy.

$\nu=0.82,0.86$] and in agreement with experimental results [25] conducted in densely packed systems. Most interesting is the behavior at the transition point: When $\nu=\nu_c$ the system oscillates between a solidlike ''jammed'' state [Fig. 1 ($t1$)] and a gaslike behavior [Figure 1 ($t2$)]: The values of Z, σ, and N (Fig. 3) fluctuate between values characteristic of the two phases. Although we discuss here average values of variables, in the low-density regime most of the shear strain was concentrated in a boundary layer, in which the density was markedly less than the system average. For $\nu>\nu_c$ the density and shear strain had much less spatial variability.

The relation between stress and strain rate is another property that changes across the phase boundary. Figure 5 shows results from simulations where the same grain configuration was sheared at different strain rates, with the top wall velocity varying between 10^{-5} to 10^{-1} of the acoustic wave speed. When $\nu<\nu_c$ time-averaged shear stress (and normal stress, not shown here) on the wall is proportional to v^2, as expected from theory [4] and experiments [7] for the ''gaslike'' granular state. When $\nu>\nu_c$ measured average stresses are nearly independent of strain rate, as expected for elastic-plastic materials and as seen in experiments in densely packed granular systems [26]. For $\nu=\nu_c$ stress-strain-rate curves resemble those of plastic materials, since high stresses in jammed states dominate the time-averaged behavior.

B. Constant force boundary condition

In this section we demonstrate the role of the critical solid fraction when the system is allowed to evolve to it's own preferred density. Soil mechanists have long known of a ''critical density.'' If a granular aggregate is overconsolidated and sheared under CFBC, it will deform while shearing and expand to this ''critical density.'' If it is initially underconsolidated it will compact while shearing until it reaches the same critical density. In systems where the deformation is concentrated into shear bands, the overall density is irrelevant but the solid fraction within the shear band approaches the critical value [27]. Although the existence of a critical density is known, it's origin has not been understood. Here we investigate this criticality, by performing simulations with a constant applied confining normal stress N_e on the rigid boundaries (CFBC), while shearing the upper wall at velocity v. Under these boundary conditions, in contrast with CVBC, the solid fraction becomes a free variable.

The simulation systems expanded or contracted during shear, depending on the initial solid fraction ν_i, and the applied confining stress N_e, to finally reach a steady state where ν, σ, and Z fluctuate around constant values. Figure 6 shows typical evolution of the systems solid fraction as it approaches and maintains a steady-state during shear. Average values of steady-state solid fractions $\langle\nu\rangle$ are plotted in Fig. 7(a) as function of N_e and v, for simulations with $\mu=0.5$. For a wide range of confining normal stresses N_e (range widens with decreasing velocity) systems attain the critical volume fraction for frictional grains, i.e., $\langle\nu\rangle\approx\nu_{c0.5}=0.805$. For frictionless disks, simulations converge on $\langle\nu\rangle\approx\nu_{c0}=0.835$, in a similar manner. Though $\langle\nu\rangle$ is fairly constant with N_e in the ''critical regime,'' the mean steady-state coordination number $\langle Z\rangle$ increases with N_e [Fig. 7(b)].

In the CFBC simulations the system does not oscillate between gas and solid phases as in CVBC, since ''jamming'' episodes may be avoided by slight dilation (producing fluctuations around the mean porosity and height). Instead, the critical state in CFBC is marked by spatial coexistence of the two phases. However, unlike simulations which include gravity, where the phases separate into different regions of the domain [14], here they are intermingled: stress-bearing chains separating ''islands'' of unstressed gas. In those sys-

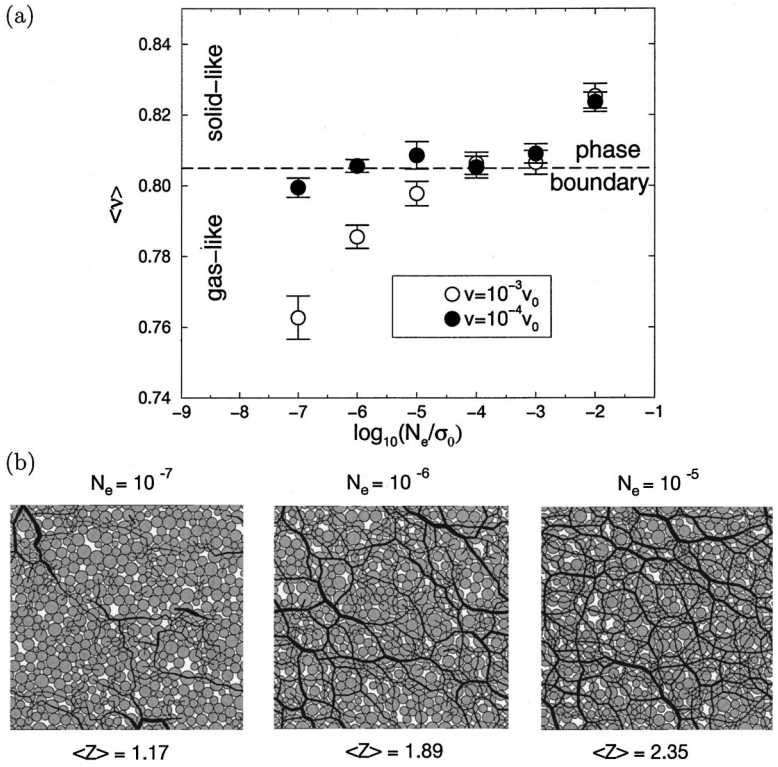

FIG. 7. (a) Time averaged steady-state solid fraction $\langle \nu \rangle$ for 24×24 systems, with $\mu=0.5$, sheared at two different velocities v, under CFBC, plotted against the confining normal stress N_e used for boundary condition. Error bars depict standard deviation from steadystate. (b) Instantaneous grain configurations and stresses for three of the $v=10^{-4}$ runs in (a). The confining stress used for each is written above the frames, and the temporally averaged coordination number is written below. Although the three runs have nearly identical solid fractions [see (a)], $\langle Z \rangle$ increases dramatically, also observed visually as increasing density of stress chains.

tems having $\langle \nu \rangle \approx \nu_c$ system-spanning stress chains begin to form. With increasing N_e, the number and size of gas islands decreases, and the connectivity of chains increases, and thus $\langle Z \rangle$ increases [Fig. 7(b)]. A measure of the amount of grains participating in chains is plotted in Fig. 8, where the fraction of grains with a coordination number greater than 2, i.e., grains that are part of a stress-supporting chain, is plotted against the applied normal load. For systems with a density near ν_c, this fraction increases slowly over a wide range of N_e. The number of stress-supporting grains increases sharply at higher normal stresses, coinciding with a transition in the solid fraction to $\nu > \nu_c$. The fact that stress in granular aggregates may be supported in a bimodal (two-phase) fashion was recently quantified in modeling of ''quasistatic'' deformation of granular systems, using CFBC [28].

Deviations of the solid fraction from its phase boundary value occur in two cases. (1) At high normal stresses, ''solidification'' occurs: $\langle \nu \rangle$ increases above ν_c, islands virtually vanish and chains become highly connected [$N_e=10^{-2}$ in Fig. 7(a), and in Fig. 8]. (2) When the ratio of inertial to normal forces is high (higher velocities and lower normal stresses), the velocity fluctuations of grains produce a ''granular pressure'' [4] which may cause decompaction, and $\langle \nu \rangle$ becomes less than ν_c: Fig. 7(a), $v=10^{-3}$ and $N_e \leqslant 10^{-5}$. In this case islands grow to divide stress chains at a region close to the shearing wall, resulting in ''fluidization'' near the wall. We also observed the gas to solid transition in the power spectra $S(\omega)$ obtained from the stress fluctuations measured on the wall $\sigma(t)$, where $S(\omega)$ varies as ω^{η} with η decreasing continuously from $\eta \sim 0$ for $N_e=10^{-7}$ to $\eta \sim -2$ for $N_e \geqslant 10^{-2}$, Fig. 9.

Why is the transition density between gas and solid also the critical density to which the system is attracted? The gaslike phase will only occur when granular pressure, which results from energy input from the boundary [4], is large enough to counterbalance the confining normal stress N_e. With increasing N_e, increasingly large flux of energy is needed to sustain the gaslike state. A loosely packed system subjected to a finite normal stress and sheared at small enough velocities will thus tend to compact and approach ν_c from below. On the other hand systems with $\nu > \nu_c$ are characterized by finite deformation (>1%) of grains, which require extremely high stresses for stiff natural granular material. Thus ν_c is the rigid limit, where stresses are accommodated by efficient load bearing structures which leave the bulk of the material free to flow. The presence of gas islands allows stress chains to form, evolve and die more easily, without jamming the system for long periods.

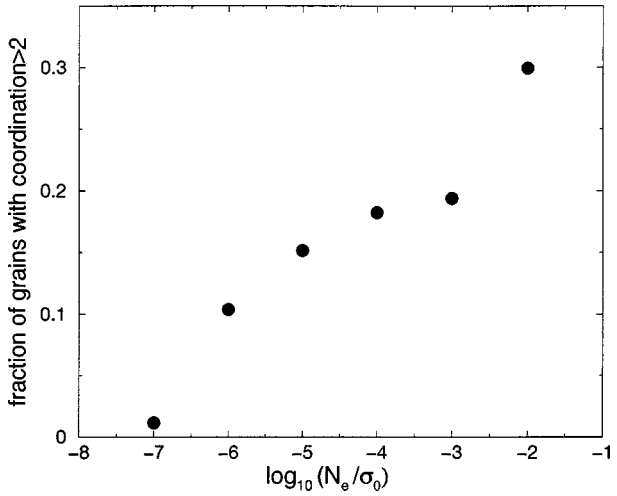

FIG. 8. Fraction of grains with coordination number greater than 2, i.e., grains participating in stress supporting chains, as function of applied normal stress N_e. Simulations use CFBC and shearing rate is $v=10^{-4}v_0$.

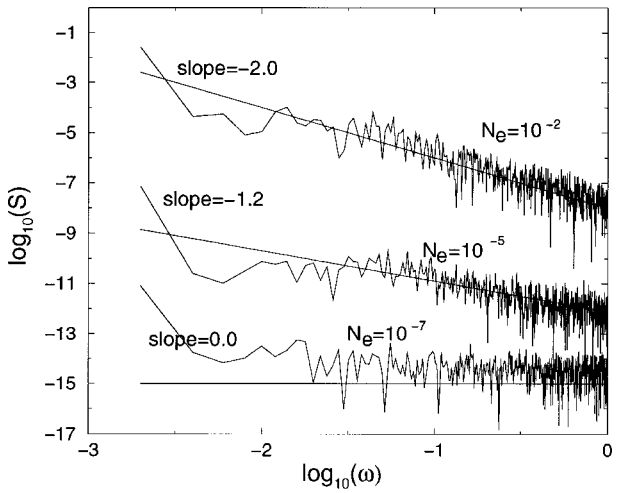

FIG. 9. Power spectra $S(\omega)$ from $\sigma(t)$, as function of frequency of stress fluctuations ω, for three 24×24 simulations initiated with same grain configuration, but sheared while using different values of applied normal stress N_e. All systems sheared at velocity $v=10^{-4}$ under CFBC, with $\mu=0.5$.

IV. CONCLUSION

To summarize, we identified a rigidity transition. The solid fraction at the transition in our experiments varied from $\nu_c=0.80-0.84$, with the lower number representing frictional grains. The critical solid-fraction is a phase-boundary between gas and elastic-plastic solid regimes of behavior. The characteristics we observe suggest that the granular rigidity transition is a first-order transition in two dimensions. However the elastic constants, as in central-force network percolation models, have second order characteristics [22]. Recent work with bond-diluted lattices [24] has shown that while the elastic constants undergo a second-order transition, the probability of a grain belonging to the infinite cluster at the rigidity transition undergoes a first-order transition. This offers an explanation for the discontinuous increase in the coordination yet a continuous increase in shear modulus in our simulations [Figs. 2(a) and 2(c)].

At the transition, we observe that the two phases coexist in space [Fig. 7(b)] and/or time (Fig. 3). The phase boundary is attractive, and corresponds to the ''critical density'' known (but previously not understood) in soil mechanics: Sheared aggregates tend to this critical volume fraction under a wide range of normal loads. Experimentally, a coexistence of gas and solid regimes has been observed in shearing granular systems [10], and oscillations between ''jamming'' and ''flowing'' states occur spontaneously in a variety of systems, from hoppers to natural and experimental land slides [29], suggesting proximity of these systems to the phase boundary. An attracting phase boundary may also explain ''fragile materials,'' a term recently used to describe 'jammed' states which may be unjammed by small fluctuations [30].

We used normal stresses ranging between $10^{-2}-10^{-7}$, which using a characteristic Young's modulus for Earth materials (e.g., rock), translates to $N_e=3-3\times10^5$ KPa, (corresponding for soils to burial depth of 0.1 m–10 km). Based on this, we suggest that many natural granular deformation processes, including the deformation that occurs in gouge filled faults during earthquakes, will occur at a local solid fraction which constitutes a phase boundary, and neither gas nor elastoplastic descriptions will fully capture these systems' behavior. However, such criticality in natural systems is easily missed, since spatial and temporal averages of stresses tend to be dominated by stress chains, and thus have the mark of solid deformation. It is clear that much more theoretical and experimental work needs to be done, including investigating much larger systems, and examining the critical state more closely.

ACKNOWLEDGMENT

This work was funded by NSF Grant No. EAR-9804855, and a grant from the Center for Non-Linear Earth Systems of the Columbia Earth Institute. We wish to thank C. Scholz and B. Shaw for helpful conversations.

[1] M. Jaeger, S. R. Nagel, and R. P. Behringer, Science **255**, 1523 (1992).
[2] O. Reynolds, Philos. Mag. **20**, 469 (1885).
[3] R. A. Bagnold, Proc. R. Soc. London, Ser. A **225**, 49 (1954).
[4] P. K. Haff, J. Fluid Mech. **134**, 401 (1983).
[5] C. K. K. Lun, S. B. Savage, D. J. Jeffrey, and N. Chepurnity, J. Fluid Mech. **140**, 223 (1984).
[6] P. A. Vermeer, Geotechnique **40**, 223 (1990).
[7] S. B. Savage and M. Sayed, J. Fluid Mech. **142**, 391 (1984).
[8] D. M. Hanes and D. L. Inman, J. Fluid Mech. **150**, 357 (1985).
[9] O. J. Schwartz, Y. Horie, and M. Shearer, Phys. Rev. E **57**, 2053 (1998).
[10] T. G. Drake, J. Geophys. Res. **95**, 8681 (1990).
[11] S. B. Savage, J. Fluid Mech. **377**, 1 (1998).
[12] C. T. Veje *et al.*, in *Physics of Dry Granular Material*, edited by S. L. H. J. Hermann and J. P. Hovi, Vol. 350 of *NATO Advanced Study Institute* (Kluwer, Netherlands, 1998), pp. 232–233.
[13] Y. Zhang and C. Campbell, J. Fluid Mech. **237**, 541 (1992).
[14] P. A. Thompson and G. S. Grest, Phys. Rev. Lett. **67**, 1751 (1991).
[15] P. A. Cundall and O. D. Strack, Geotechnique **29**, 47 (1979).
[16] H. Tillemans and H. J. Herrmann, Physica A **217**, 261 (1995).
[17] M. P. Allan and D. J. Tildesley, *Computer·Simulation of Liquids* (Oxford University Press, Oxford, 1987).
[18] C. S. Campbell and C. E. Brennen, J. Fluid Mech. **151**, 167 (1985).
[19] D. Bideau and J. P. Troadec, J. Phys. C **17**, L731 (1984).
[20] D. Durian, Phys. Rev. Lett. **75**, 4780 (1995).
[21] K. Walton, J. Mech. Phys. Solids **35**, 213 (1987).
[22] E. Guyon *et al.*, Rep. Prog. Phys. **53**, 373 (1990).
[23] S. P. Obukhov, Phys. Rev. Lett. **74**, 4472 (1995).
[24] C. Moukarzel, P. M. Duxbury, and P. L. Leath, Phys. Rev. Lett. **78**, 1480 (1997).

[25] B. Miller, C. O'Hern, and R. Behringer, Phys. Rev. Lett. **77**, 3110 (1996).
[26] C. Marone, B. E. Hobbs, and A. Ord, Pure Appl. Geophys. **139**, 195 (1992).
[27] J. Desrues, R. Chambon, M. Mokni, and F. Mazerolle, Geotechnique **46**, 529 (1996).
[28] F. Radjai, D. E. Wolf, M. Jean, and J. J. Moreau, Phys. Rev. Lett. **80**, 61 (1998).
[29] J. Major, J. Geol. **105**, 345 (1997).
[30] M. Cates, J. Wittmer, J. Bouchaud, and P. Claudin, Phys. Rev. Lett. **81**, 1841 (1998).